FROM BFKL TO THE SOFT POMERON: AN ATTEMPT TO FIND AN INTERPOLATION*

Jochen Bartels

II. Institut für Theoretische Physik, Universitaet Hamburg, Germany

(Received March 5, 2019)

We describe an attempt to use the renormalization group equations for interpolating between the BFKL Pomeron in perturbative QCD and the soft Pomeron in pp scattering.

DOI:10.5506/APhysPolBSupp.12.765

1. Introduction

The high-energy behavior of elastic proton–proton scattering has always been a topic of high interest. In particular, in recent years, the LHC has provided new data which have stimulated attempts to find a theoretical description. Up to today, there is no theory based upon QCD which allows access to this nonperturbative hadron–hadron scattering process.

In perturbative QCD high-energy scattering processes, in the simplest approximation, are described by the BFKL Pomeron, a bound state of two (reggeized) gluons: it applies to the scattering of small-size objects, such as highly virtual photons or jet production with large rapidity gaps (Mueller–Navelet jets). The cross section of these processes exhibits a rise with energy, resulting from the BFKL intercept above one. At asymptotic energies, it is expected that this BFKL description will require unitarity corrections. On the other hand, in proton–proton scattering, transverse sizes are of the order of the proton radius and thus the scattering amplitude becomes nonperturbative. Successful descriptions are based upon phenomenological Regge models, *e.g.* the well-known soft Pomeron of Donnachie and Landshoff with intercept much closer to unity than the perturbative BFKL Pomeron. Recent LHC data have also stimulated discussions whether, in addition to the Pomeron with even C-parity, there exists also a C-odd exchange, the so-called odderon which should manifest itself in differences of the cross

* Presented at the Diffraction and Low-x 2018 Workshop, August 26–September 1, 2018, Reggio Calabria, Italy.

sections when comparing proton–proton and proton–antiproton scattering. Interesting enough, on the perturbative side an odderon exists, as a bound state of three (reggeized) gluons.

It appears tempting to search for a connection between the perturbative BFKL Pomeron, valid for small transverse distances, and the nonperturbative soft Pomeron governed by larger transverse distances in the confinement region. In quantum field theory, the renormalization group provides a bridge between different momentum (or distance) scales. For practical calculations, the exact renormalization group equations (RGE, Wetterich equations [1, 2]) offer a convenient formulation which is now widely being used, *e.g.* in solid state physics, gravity or in QCD.

Some time ago, we have started [3–5] an attempt to make use of this RGE formalism for finding a bridge between the perturbative (UV) region and the nonperturbative (IR) region. In the first step, we have investigated the IR region: in this region, we make use of (local) Reggeon Field Theory, and we have studied the fixed point structure of different theories containing Pomeron and/or odderon fields. More recently [5], we have begun to address the UV region. First results of this UV study will be presented in this paper.

2. RG equation of the BFKL Green's function

Let me first give a general overview about this part of our program. The starting point is QCD. However, instead of beginning with the standard QCD Lagrangian, we make use of the high-energy description of QCD developed by Lipatov, the so-called effective action [6]. The essential new ingredient is the reggeized gluon which, in QCD at high energies, replaces the elementary gluon exchange. Based upon this effective action, we formulate an effective field theory in $2+1$ dimensions. It contains fields for the reggeized gluon which propagate in rapidity, as well as elementary gluons which are local in rapidity. This field theory allows to derive the leading order BFKL Pomeron as a bound state of two reggeized gluons. After the introduction of an IR regulator

$$\frac{1}{\boldsymbol{q}^2} \;\to\; \frac{1}{\boldsymbol{q}^2 + R_k\left(\boldsymbol{q}^2\right)}\,, \tag{1}$$

$$R_k\left(\boldsymbol{q}^2\right) \;=\; \left(k^2 - \boldsymbol{q}^2\right)\Theta\left(k^2 - \boldsymbol{q}^2\right)\,, \tag{2}$$

which suppresses the low-momentum region. This effective field theory can be used to formulate RG equations. Without further approximations, we first find a differential equation for the derivative of the (IR regulated) leading order BFKL Pomeron with respect to the cutoff parameter k. Diagrammatically, this equation can be formulated as in Fig. 1. It has the form of the nonlinear infrared evolution equations derived by Lipatov and Kirschner [7].

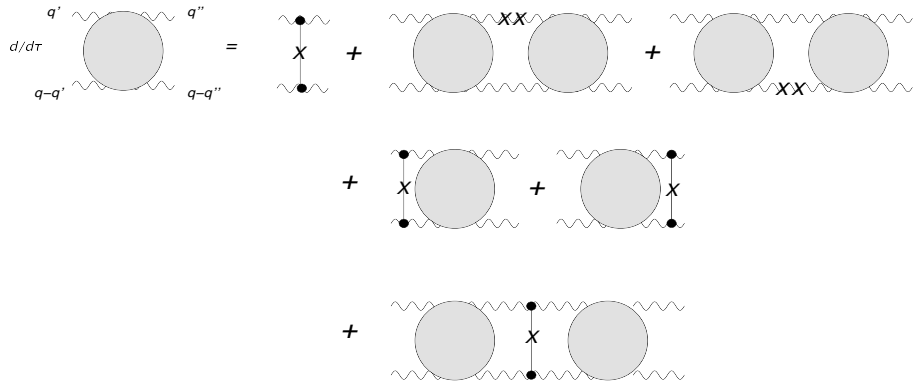

Fig. 1. Derivative of the BFKL ladder w.r.t. the cutoff.

In [5], it is then shown that the same equation can be derived from the flow equations [1, 2]

$$k\frac{\partial}{\partial k}\Gamma_k = \frac{1}{2}\mathrm{Tr}\left[\left(\Gamma_k^{(2)} + R_k\right)^{-1} k\frac{\partial}{\partial k}R_k\right] . \tag{3}$$

Using our effective field theory mentioned before and taking functional derivatives with respect to the gluon fields, one arrives at an infinite set of coupled flow equations. Then, by employing special identities of vertex function, one derives — without further truncations — closed two-loop equations. One of them is the equation for the four point function, the BFKL Green's function illustrated above. This result implies that the BFKL Pomeron satisfies the flow equations. In practice, however, it may be more convenient, rather than solving the set of flow equations, to make use of the nonlinear differential equation which has been shown to be equivalent to the set of flow equations.

In the next step, we introduce the triple Pomeron vertex. For this, the effective field theory described before has to be generalized such that it allows for the $2 \to 4$ transition vertex of reggeized gluons (Fig. 2 (a)).

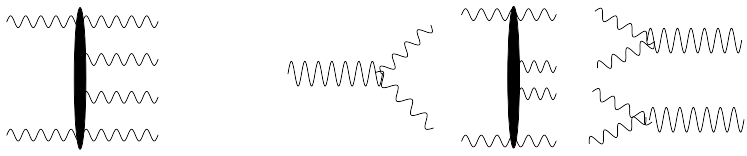

(a) (b)

Fig. 2. The triple Pomeron vertex: (a) the $2 \to 4$ transition vertex of reggeized gluons, (b) convolution with bound state Pomeron fields.

This transition vertex, in momentum space, has first been derived in [8] and further investigated in, *e.g.*, [9]. After transformation to coordinate space, it has been shown to coincide with the kernel of the BK-equation.

For the study of the impact of this triple Pomeron vertex, it becomes much more convenient to switch, from our effective field theory which is formulated in terms of gluon fields, to Reggeon Field Theory of the bound state of two reggeized gluons. They are obtained from the eigenstates ψ_n of the BFKL kernel, and their intercepts are given by the eigenvalues ω_n

$$\begin{aligned} \mathcal{G}_k &= \frac{1}{\omega - \tilde{K}_k} \\ &= \sum_n \frac{\psi_{n,k}\left(\boldsymbol{q}', \boldsymbol{q} - \boldsymbol{q}'\right) \psi^*_{n,k}\left(\boldsymbol{q}'', \boldsymbol{q} - \boldsymbol{q}''\right)}{\omega - \omega_{n,k}} + \text{continuous part}\,. \end{aligned} \tag{4}$$

(Here, the subscript k denotes the dependence upon the cutoff parameter.) These Pomeron fields, together with their interactions, define a local Reggeon Field Theory which can further be studied by the methods outlined in our earlier papers [3, 4]. The most important interaction is given by the triple Pomeron vertices: in our bound state formulation, they are obtained by convoluting the $2 \to 4$ transition vertex of reggeized gluons with the Pomeron bound state wave functions (Fig. 2 (b)).

3. Numerical analysis of the spectrum of the regulated BFKL equation

In order to further proceed along these lines, we need to study numerically the eigenvalue spectrum of the BFKL kernel, with the IR regulator included in the momentum propagators and the fixed QCD coupling α_s being replaced by the running coupling

$$\bar{\alpha}_\mathrm{s}\left(\boldsymbol{q}^2\right) = \frac{N_\mathrm{c}}{\pi} \frac{3.41}{\beta_0 \ln\left(\boldsymbol{q}^2 + R_0^2\right)}\,. \tag{5}$$

For illustration, we present the regulated kernel in the forward direction

$$\tilde{K}\left(\boldsymbol{k}, \boldsymbol{k}'\right) = K_\mathrm{BFKL}\left(\boldsymbol{k}, \boldsymbol{k}'\right) + 2\delta^{(2)}\left(\boldsymbol{k} - \boldsymbol{k}'\right) \omega_g\left(\boldsymbol{k}^2\right) \tag{6}$$

with

$$K_\mathrm{BFKL}\left(\boldsymbol{k}', \boldsymbol{k}''\right) = \frac{\bar{\alpha}_\mathrm{s}}{2\pi} \frac{\boldsymbol{k}'^2}{D\left(\boldsymbol{k}'\right)} \frac{2}{D\left(\boldsymbol{k}' - \boldsymbol{k}''\right)} \frac{\boldsymbol{k}''^2}{D\left(\boldsymbol{k}''\right)} \tag{7}$$

and

$$\omega_{g,k}\left(\boldsymbol{q}^2\right) = -\boldsymbol{q}^2 \frac{\bar{\alpha}_\mathrm{s}}{4\pi} \int \mathrm{d}^2\boldsymbol{l} \frac{1}{D(\boldsymbol{l}) D(\boldsymbol{q} - \boldsymbol{l})}\,, \tag{8}$$

where

$$\begin{aligned} D(\boldsymbol{q}) &= \boldsymbol{q}^2 + R_k\left(\boldsymbol{q}^2\right) \\ &= k^2\Theta\left(k^2 - \boldsymbol{q}^2\right) + \boldsymbol{q}^2\Theta\left(\boldsymbol{q}^2 - k^2\right) . \end{aligned} \tag{9}$$

For this kernel, we have computed eigenvalues, eigenfunctions and slopes (the latter quantities are obtained by expanding the BFKL kernel in powers of the momentum transfer $\boldsymbol{q}^2$), for different values of the IR cutoff k. Calculations are done by discretizing the momentum integrations. Details are found in [5]; here, we only summarize the main features.

(a) The eigenvalues: as it is well known, the spectrum of the leading order BFKL Pomeron without IR cutoff and running coupling consists of a fixed cut in the ω plane which runs from the positive value $\omega_{\mathrm{BFKL}} = 4\ln 2\frac{\alpha_s N_c}{\pi}$ to $-\infty$. Several attempts of introducing an infrared cutoff and the running coupling (*e.g.* with the Higgs mechanism [10, 11], infrared boundary values [12, 13]) lead to the same modification of this picture: on the positive side of the ω axis, the cut is replaced by an infinite number of discrete poles which accumulate at $\omega = 0$. On the negative ω axis the cut remains. Our calculations have the same pattern, and we have computed the leading eigenvalues ω_n for $n = 1, \ldots, 16$ (see Fig. 3).

The n-dependence of these eigenvalues is approximately given by (for $k = 1$ GeV).

$$\omega_n \approx \frac{1}{0.052 + 2.24\, n} . \tag{10}$$

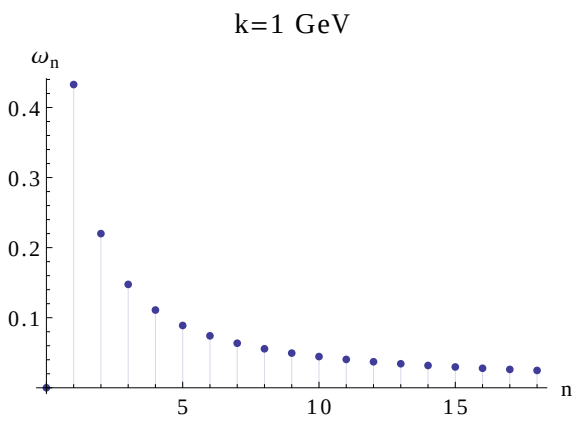

Fig. 3. Intercepts of the leading discrete Pomeron states.

(b) Only the first leading eigenfunction ($n = 1$) has its main support in the region of small momenta. With increasing n, the support very quickly moves into the UV-region. Defining for each state a (logarithmic) radius $R_n = \langle \ln q^2 \rangle$ we find a linear growth with n. In detail, for $k = 1$ GeV we find for the first three eigenstates the radii $R_1 = 4.7$ GeV, $R_2 = 1.2 \times 10^2$ GeV, and $R_3 = 3.3 \times 10^3$ GeV. This implies that only the state with $= 1$ can be named "soft", whereas all others are "hard".

(c) The slopes α'_n go to zero rapidly with increasing n

$$\frac{1}{153.11 + 23.342\, n^2} \tag{11}$$

(again, for $k = 1$ GeV).

(d) Increasing the IR cutoff k, we find that the eigenvalues and slopes become smaller, whereas the radii increase.

4. Conclusions

We are now facing the most interesting question: what happens to this infinite number of Pomeron states of the BFKL Pomeron once the interaction between the Pomeron fields is included, in particular how do the Pomeron loops generated by the triple Pomeron vertices affect the free BFKL states? In order to find answers to these questions, we first will compute the numerical values of the triple Pomeron vertices (*cf.* Fig. 2 (b)), and then use this as input to a RFT flow analysis, as prepared in [3, 4]. Work along these lines is in progress.

REFERENCES

[1] C. Wetterich, *Phys. Lett. B* **301**, 90 (1993).

[2] T.R. Morris, *Phys. Lett. B* **329**, 241 (1994) [arXiv:hep-ph/9403340].

[3] J. Bartels, C. Contreras, G.P. Vacca, *J. High Energy Phys.* **1603**, 201 (2016) [arXiv:1512.07182 [hep-th]].

[4] J. Bartels, C. Contreras, G.P. Vacca, *Phys. Rev. D* **95**, 014013 (2017) [arXiv:1608.08836 [hep-th]].

[5] J. Bartels, C. Contreras, G.P. Vacca, *J. High Energy Phys.* **2019**, 4 (2019) [arXiv:1808.07517 [hep-ph]].

[6] L.N. Lipatov, *Nucl. Phys. B* **452**, 369 (1995) [arXiv:hep-ph/9502308].

[7] R. Kirschner, L.N. Lipatov, *Sov. Phys. JETP* **56**, 266 (1982) [*Zh. Eksp. Teor. Fiz.* **83**, 488 (1982)].

[8] J. Bartels, M. Wusthoff, *Z. Phys. C* **66**, 157 (1995).

[9] J. Bartels, L.N. Lipatov, G.P. Vacca, *Nucl. Phys. B* **706**, 391 (2005) [arXiv:hep-ph/0404110].

[10] M. Braun, G.P. Vacca, G. Venturi, *Phys. Lett. B* **388**, 823 (1996) [arXiv:hep-ph/9605304].

[11] E. Levin, L. Lipatov, M. Siddikov, *Phys. Rev. D* **89**, 074002 (2014) [arXiv:1401.4671 [hep-ph]]; *Eur. Phys. J. C* **75**, 558 (2015) [arXiv:1508.04118 [hep-ph]]; *Phys. Rev. D* **94**, 096004 (2016) [arXiv:1608.03816 [hep-ph]].

[12] L.N. Lipatov, *Sov. Phys. JETP* **63**, 904 (1986) [*Zh. Eksp. Teor. Fiz.* **90**, 1536 (1986)].

[13] H. Kowalski, L. Lipatov, D. Ross, *Eur. Phys. J. C* **74**, 2919 (2014) [arXiv:1401.6298 [hep-ph]]; *Eur. Phys. J. C* **76**, 23 (2016) [arXiv:1508.05744 [hep-ph]]; H. Kowalski, L.N. Lipatov, D.A. Ross, O. Schulz, *Eur. Phys. J. C* **77**, 777 (2017) [arXiv:1707.01460 [hep-ph]].